JOURNAL OF CATALYSIS 38, 206–213 (1975)

Adsorption of Sulfur Dioxide on Silica Gel— Rate and Equilibrium Parameters

M. A. GALAN[1] AND J. M. SMITH

University of California, Davis, California 95616

Received October 23, 1974

A pulse-response (chromatographic) method was used to measure adsorption and intraparticle mass transfer properties of sulfur dioxide in silica gel particles at 175 to 270°C and 1 atm pressure. Adsorption was reversible in the 175–270°C range but nearly irreversible, in the time period of the chromatographic experiments, below 150°C.

The heat of adsorption (−6.5 kcal/mole) and adsorption rate constants indicated that at 175 to 270°C the SO_2 molecules were held on the silica gel sites with bonds of intermediate strength.

Intraparticle mass transfer significantly affected the overall rate of adsorption for all particles with radii larger than 0.1 mm. Hence, this resistance should be considered in designing equipment for removal of SO_2 from gases, unless the particle size is very small. Surface and pore-volume diffusion appear to contribute about equally to the intraparticle diffusivity.

NOMENCLATURE

C	concentration of SO_2 in the gas, mole/cm^3
C_s	adsorbed concentration of SO_2, moles/(cm^3 of particle volume)
D_e	effective intraparticle diffusivity, cm^2/sec
D_s	effective surface diffusivity, cm^2/sec
$\mathscr{D}_{SO_2-He}$	molecular diffusivity, cm^2/sec
$\mathscr{D}_K$	Knudsen diffusivity, cm^2/sec
E	activation energy, kcal/mole
E_A	axial dispersion coefficient, based on cross-sectional area of column, cm^2/sec
ΔH	heat of adsorption, kcal/mole
k_{Ad}	adsorption rate constant, cm^3/(g)(sec)
k_f	mass transfer coefficient from gas to particle surface, cm/sec
K_A	adsorption equilibrium constant, cm^3/g
l	scale of dispersion, cm
L	length of bed, cm
n	adsorbed concentration of SO_2, mole/g
R	average radius of silica gel particles (assumed spherical), cm
t	time, sec
t_0	injection time of pulse, sec
T	temperature, °K
v_0	superficial gas velocity in bed, cm/sec
v	gas velocity in the void space of the bed, cm/sec
z	axial distance from inlet of bed, cm
α	void fraction in the bed
β	intraparticle void fraction
δ_0, δ_1	moment contributions defined by Eqs. (3) and (4)
η	diffusibility
μ	gas viscosity, g/(cm)(sec)
μ_1	first absolute moment, sec
$(\mu_1)_d$	first absolute moment in dead volume, sec
$(\mu_1)_{inert}$	first absolute moment for helium pulses in nitrogen, sec
μ_2'	second central moment, sec^2

[1] On leave from University of Salamanca, Spain.

ρ_p apparent particle density, g/cm³
τ_a apparent tortuosity factor
τ tortuosity factor for pore-volume diffusion

The design of equipment for removal of sulfur dioxide from gases by adsorption and desorption requires equilibrium and rate information. Silica gel has a relatively high adsorption capacity for SO_2 yet its adsorption characteristics have not received much attention. Equilibrium isotherms have been measured by Jones and Ross (*1*) from −10 to 50°C. No rate data for the adsorption process, including intraparticle diffusivities and intrinsic rate constants at the adsorption site, have been reported. The objectives of the present study were to determine these rate parameters by applying the chromatographic technique (*2*) in a fixed bed of silica gel particles.

As indicated in the Experimental Procedures Section, desorption at temperatures below about 150°C is slow. One of the requirements of the chromatographic theory applied here is that the adsorption be reversible within the time period of the experiment. Hence, the measurements were made from 175 to 270°C at nearly atmospheric pressure. The model used to interpret the data takes into account axial dispersion in the void space of the bed as well as mass transfer from the gas to particle. Experiments were made at different gas flow rates in order to separate these two effects from intraparticle diffusion and adsorption at an interior site.

METHOD

Each experiment consisted of injecting a pulse of gas containing SO_2 (in helium as carrier gas) into the bed and analyzing the measured concentration vs time peak in the bed effluent. If the adsorption rate is linear and reversible, adsorption equilibrium and rate parameters can be extracted from the difference between the first-absolute and second-central moments of the inlet pulse and the effluent peaks. Based upon the model described and other secondary assumptions, Schneider and Smith (*2*) have presented the following equations relating these moment differences to the equilibrium and rate parameters (K_A, E_A, D_e, k_f, and k_{Ad}):

$$\mu_1 - \frac{t_0}{2} = (\mu_1)_d + \frac{z}{v}\left[1 + \frac{1-\alpha}{\alpha}(\beta + \rho_p K_A)\right], \tag{1}$$

$$\mu_2' - \frac{t_0^2}{12} = (\mu_2')_d + \frac{2z}{v}\left[\frac{E_A}{\alpha}\frac{(1+\delta_0)^2}{v^2} + \delta_1\right], \tag{2}$$

where

$$\delta_0 = \frac{1-\alpha}{\alpha}\beta\left[1 + \frac{\rho_p}{\beta}K_A\right], \tag{3}$$

$$\delta_1 = \frac{1-\alpha}{\alpha}\beta\left[\frac{\rho_p}{\beta}\frac{K_A^2}{k_{Ad}} + \frac{R^2\beta}{15}\left(1 + \frac{\rho_p}{\beta}K_A\right)^2\left(\frac{1}{D_e} + \frac{5}{k_f R}\right)\right]. \tag{4}$$

Values of the first-absolute and second-central moments were calculated from the measured effluent peaks by the expressions:

$$(\mu_1) = \frac{\int_0^\infty t\,C(L,t)\,dt}{\int_0^\infty C(L,t)\,dt}, \tag{5}$$

$$\mu_2' = \frac{\int_0^\infty (t-\mu_1)^2\,C(L,t)\,dt}{\int_0^\infty C(L,t)\,dt}, \tag{6}$$

where $C(L,t)$ is the concentration peak at the exit of the bed. The data for different

velocities and particle sizes were sufficient to determine K_A, D_e and k_{Ad}, as described below. The results at different temperatures were used to evaluate the heat and activation energy of adsorption.

Experimental Procedures

The apparatus consisted of a gas chromatograph, with thermal conductivity detector, in which the separation column contained the bed of silica gel particles. A flow diagram and details of the apparatus were given by Schneider and Smith (*2*).

Tables 1 and 2 give the properties of the silica gel (Grade 40, Davison Chemical Co.) and the properties of the columns used.

Prior to the runs each bed was pretreated with a flow (20–30 cm³/min) of pure helium at 330°C for 18–20 hr. Preliminary measurements were made to determine the adsorption characteristics of the system at various temperatures. Successive pulses of 1.0 cm³ volume (25°C, 1 atm) containing 3.0 mole% SO_2 in helium were introduced at increasing temperatures, starting at 30°C. At 150°C a very flat concentration vs time peak in the effluent gas was observed. At lower temperatures, between 30 and 150°C, no effluent peak was detectable. At a temperature of about 175°C the response peak was very large, indicating that the accumulated adsorption of many prior peaks was desorbed. The pulse volume was changed to 3.0 cm³ (to obtain peaks of reasonable magnitude) and injections made at temperatures from 175 to 270°C. In this temperature range the response peaks were well-shaped with little tailing.

TABLE 1
PROPERTIES OF SILICA GEL PARTICLES[a]

Surface area (m²/g)	832
Void vol (cm³/g)	0.43
Particle density, ρ_p (g/cm³)	1.13
Internal void fraction β	0.486
Av pore radius (Å)	11

[a] Masamune and Smith (*3*).

TABLE 2
CHARACTERISTICS OF PACKED-BED COLUMNS

Column no.	1	2	3
Packed length (cm)	20.3	20	20
Column i.d. (mm)	7.75	7.75	7.75
Particles			
1. Mesh size range	14–16	28–32	60–65
2. Av radius (mm)	0.540	0.272	0.114
Bed void fraction, α	0.327	0.337	0.361
Temp (°C)	200, 235 270	175[a]–200 235, 270	175,[a] 200 235, 270
Gas flow rate (cm³/min)(25 °C, 1 atm)	10–150	10–150	10–150

[a] First moment measurements only.

Linearity and Reversibility Tests

Equations (1–4) are based upon a first-order and reversible rate of adsorption, according to the equation:

$$\frac{\partial n}{\partial t} = k_{Ad}\left(C - \frac{n}{K_A}\right). \qquad (7)$$

Hence, it is necessary to choose experimental conditions so that Eq. (7) is applicable. To test the linearity assumption, first moments were measured at 200°C for inlet pulses containing 3 and 5% SO_2 in helium. The 200°C results in Fig. 1 show that the first moment is independent of concentration of SO_2 in the inlet pulse. This can be true only if the adsorption isotherm at 200°C is linear from 0 to 5%.

The reversibility requirement was examined by measuring the peak areas of the effluent peaks and comparing them with areas of the inlet pulses. The latter were determined by replacing the packed bed with a short capillary tube. The results (at 200°C) in Fig. 2 show about the same areas, indicating that desorption was essentially complete during the time of the pulse-response experiment. If linear and reversible adsorption occur at 200°C, it is safe to assume that these restrictions will be met at higher temperatures.

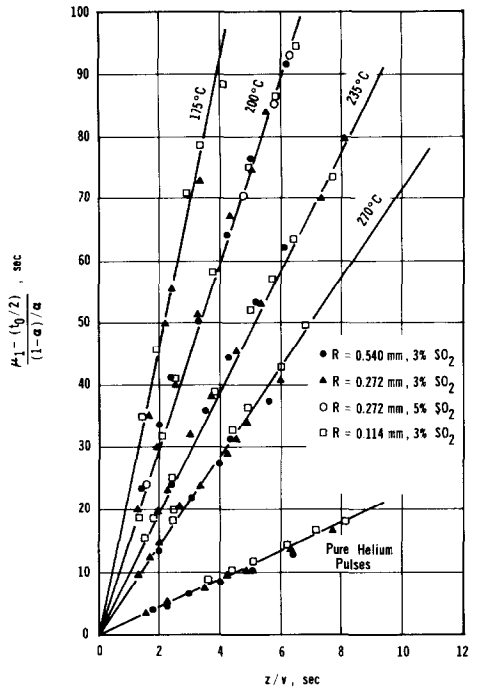

FIG. 1. First moment results.

On the basis of these tests, the final data were obtained using 3.0 cm^3 pulses of 3% SO_2 for the three particle sizes and the temperatures listed in Table 2.

First Moment Analysis

To use the first moments in Eq. (1) it is necessary to determine $(\mu_1)_d$, the retention time in the dead volumes in the lines between pulse injection and entrance to the bed and between bed exit and the detector. This was done by introducing 1.0 cm^3 pulses of pure helium, using nitrogen as a carrier gas, with the bed at 200°C. The results are shown in Fig. 1. For a nonadsorbing gas such as helium $K_A = 0$ and Eq. (1) reduces to

$$(\mu_1)_{\text{inert}} - \frac{t_0}{2} = (\mu_1)_d + \frac{z}{v}\left(1 + \frac{1-\alpha}{\alpha}\beta\right). \tag{8}$$

Then $(\mu_1)_d$ can be eliminated by subtracting Eq. (8) from Eq. (1) to give

$$\frac{\mu_1 - (t_0/2)}{(z/v)[(1-\alpha)/\alpha]} - \frac{[\mu_1 - (t_0/2)]_{\text{inert}}}{(z/v)/[(1-\alpha)/\alpha]} = \rho_p K_A. \tag{9}$$

Since K_A is independent of particle size, the first moments also should be independent of particle radius. The results for all particles, plotted in Fig. 1, show that this requirement is met reasonably well.

For application of Eq. (9), least-square analysis was used to fit straight lines to the data in Fig. 1. Then the difference between the slopes of the lines for SO_2 and for helium pulses was formulated for each temperature. According to Eq. (9), these differences in slope are equal to $\rho_p K_A$. The results for K_A are given in Table 3 and plotted vs $1/T$ in Fig. 3. The heat of adsorption corresponding to the straight line in Fig. 3 is $\Delta H = -6.5$ kcal/g. This is less than the value of -9.3 kcal/g mole reported by Jones and Ross (*1*) but their temperature range was lower (-10 to 50°C) and a different silica gel, 923 chromatographic grade (Davison Chemical Co.), was used. Ma and Marcel (*4*) found

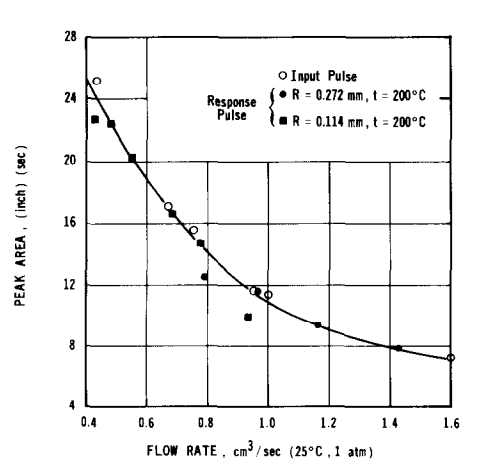

FIG. 2. Effect of adsorption on effluent peak areas; 3% SO_2–He pulses.

TABLE 3
ADSORPTION EQUILIBRIUM AND RATE CONSTANTS

t (°C)	175	200	235	270
K_A (cm^3/g)	16.3	10.9	6.9	4.3
k_{Ad}[cm^3/(g)(sec)]		20	34	61

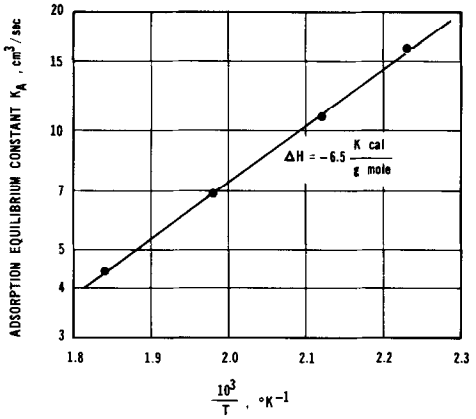

FIG. 3. Adsorption equilibrium constants for SO_2 on silica gel.

$\Delta H = -2.2$ and -2.7 kcal/g mole for adsorption of SO_2 on 5A and sodium mordenite molecular sieves. The adsorption equilibrium constants reported for the latter systems at 133 to 261°C were also less than those given in Table 3, indicating that silica gel has a higher adsorption capacity for SO_2 than does these molecular sieves. The chromatographic method used by Ma and Marcel and in the present study gives heats of adsorption corresponding to nearly zero surface coverage since the concentration of adsorbed SO_2 is very low throughout the column.

Second Moment Analysis

Axial Dispersion

Before the intraparticle diffusivity and adsorption rate constant can be extracted from the second moments, it is necessary to separate the axial dispersion contribution to μ_2'; that is, it is necessary to determine δ_1 in Eq. (2). The coefficient E_A depends upon the geometry of the bed, particularly the particle size R, and upon the gas velocity. The second moments, evaluated for various flow rates, can be used to establish the velocity dependency for each particle size. A relation between velocity and E_A can be expressed in terms of molecular and convective terms (5)

$$\frac{E_A}{\mathscr{D}_{AB}} = \eta + l\frac{v_0}{\mathscr{D}_{AB}}, \qquad (10)$$

where the diffusibility η is a measure of the molecular contribution and l, the scale of dispersion, refers to the convective contribution. Equation (2) can now be expressed in terms of η and l by using Eq. (10) for E_A:

$$\frac{\mu_2' - (t_0^2/12) - (\mu_2')_d}{2z/v} = \frac{\eta \mathscr{D}_{SO_2\text{-He}}}{\alpha v^2}(1+\delta_0)^2 + \frac{l}{v}(1+\delta_0)^2 + \delta_1. \qquad (11)$$

The second moment, $(\mu_2')_d$, in the dead volumes was measured approximately by replacing the column with a short length of capillary tubing and introducing pulses of 3% SO_2 in helium. The values of $(\mu_2')_d$ so determined were always less than 3% of the values obtained with the silica gel column. Since this is less than the accuracy of the second moments, the correction for $(\mu_2')_d$ in Eq. (11) was neglected. Figures 4-6 show the second moment results plotted according to Eq. (11). The intercepts at $1/v = 0$ of the curves on Figs. 4-6 illustrate the required values of δ_1.

To improve the accuracy of the extrapolation to $1/v = 0$, the data in Figs. 4-6 were fit to Eq. (11) using the least-square technique with η, l, and δ_1 as para-

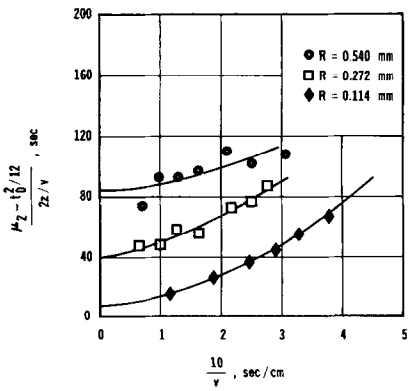

FIG. 4. Second moments at 200°C.

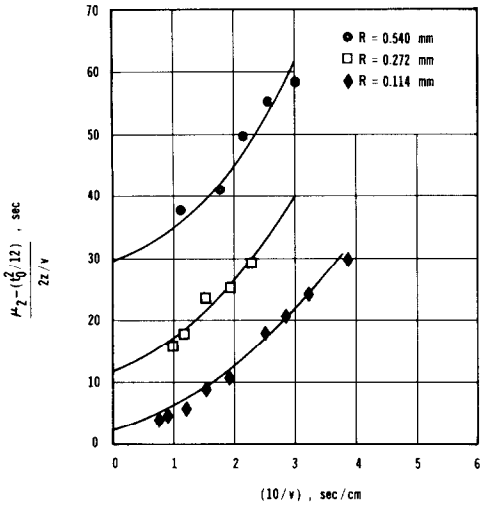

FIG. 5. Second moments for SO_2 at 235°C.

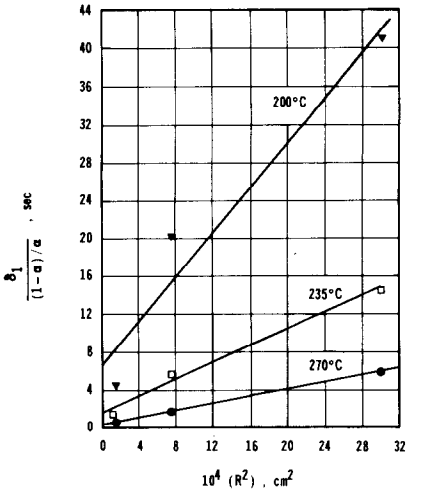

FIG. 7. Relation between $\delta_1/[(1-\alpha)/\alpha]$ and R^2.

meters. The curves in Figs. 4–6 show how the curves located in this way compare with the data. Axial dispersion in beds of small particles appears to be very sensitive to method of packing and other poorly definable characteristics of the bed (*5,6*). Hence, this procedure using moment vs velocity data is probably more accurate than estimates from available correlations for E_A.

Adsorption Rate Constants

The δ_1 values are plotted vs R^2 in Fig. 7. According to Eq. (4), these results should give a straight line with an intercept equal to $(\rho_p K_A^2/k_{Ad})$. The rate constants evaluated from these intercepts are listed in Table 3 and plotted vs $1/T$ in Fig. 8. The activation energy for adsorption obtained from Fig. 8 is about 8 kcal/g mole.

The values of k_{Ad} are approximate because of the uncertainties in the intercepts in Figs. 4–6 and 7. However, no other rate data are available for SO_2 adsorption on silica gel so that approximate results should be useful.

For comparison, Suzuki and Smith (*7*) found somewhat lower rates for the chemisorption of H_2 in a Cu·ZnO catalyst [$k_{Ad} = 4.0$ cm³/(g)(sec) 200°C]. For purely physical adsorption, Schneider and Smith (*2*) reported k_{Ad} at 50°C to be 167, 255, and 1500 cm³/(g)(sec) for C_2H_6, C_3H_8 and

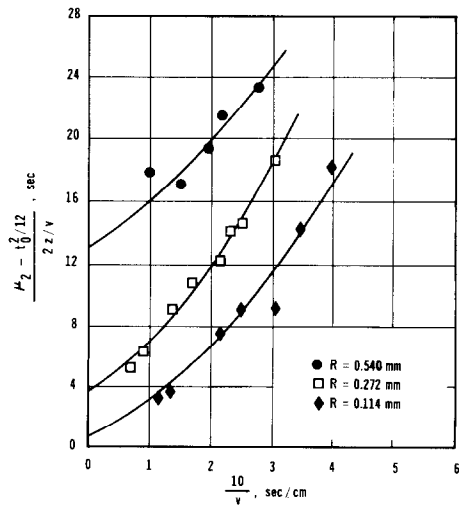

FIG. 6. Second moments for SO_2 at 270°C.

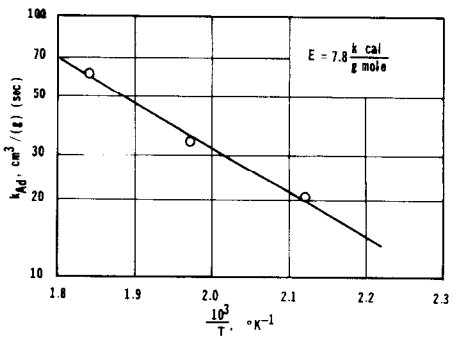

FIG. 8. Adsorption rate constants.

n-C_4H_{10}, respectively, on the same silica gel. Thus, the adsorption rate for SO_2 on silica gel is intermediate between the rate of physical adsorption of light hydrocarbons on the same silica gel and chemisorption rates of hydrogen. The activation energy given (*7*) for H_2 on Cu·ZnO was 14.6 kcal/g mole. Ma and Marcel (*4*) report 4.3 and 5.3 kcal/g mole for SO_2 adsorption on 5A and sodium mordenite molecular sieves.

Intraparticle Diffusivity

The relative large values of the ordinates with respect to the intercepts of the lines in Fig. 7 demonstrate that intraparticle diffusion is of major importance in determining the overall rate of adsorption. From Eq. (4), the slopes of the lines in Fig. 7 are a function of the combined effects of gas-to-particle mass transfer and intraparticle diffusion. Since R, β, K_A and ρ_p are known, the sum $(1/D_e + 5/k_fR)$ can be evaluated from the slopes. The results, presented in Table 4, are also approximate, particularly for 200°C, since the slope is uncertain at this temperature. As is usual for gas phase gas systems, the gas-to-particle contribution to the second moment is relatively small. This is shown by the values of $5/k_fR$ given in Table 4. They were estimated from the correlation for Sherwood numbers in packed beds given by Wakao *et al.* (*8*). The molecular diffusivity $\mathscr{D}_{SO_2\text{-He}}$ was calculated from the Chapman-Enskog equation (9).

The resultant values for the effective diffusivity were then used to determine an apparent tortuosity factor, τ_a, defined by the expression

$$D_e = \frac{\beta \mathscr{D} K}{\tau_a}. \qquad (12)$$

These values (Table 4) were about 1.5, which is lower than the expected number of about 4 (*10*) and lower than 3.35, the value determined by Schneider and Smith (*11*) for the same silica gel under nonadsorbing conditions. Such results suggest that surface diffusion is involved when SO_2 diffuses in silica gel particles. Significant surface transport frequently accompanies physical adsorption (*11*).

The relative importance of pore-volume and surface diffusion can be estimated if it is assumed that adsorption and desorption on a site are rapid with respect to surface diffusion. Under these conditions the two contributions to the effective diffusivity may be written

$$D_e = \frac{\beta \mathscr{D}_K}{\tau} + \rho_p K_A D_s, \qquad (13)$$

where τ is the tortuosity factor, 3.35, for pore-volume diffusion and D_s is a surface diffusivity. The latter is defined as the surface transport rate per unit total area perpendicular to the direction of diffusion per unit driving force, dC_s/dr. Here the concentration C_s is the moles adsorbed per unit volume of particle, or $\rho_p n$. The Knudsen diffusivity $\mathscr{D}_K$ for SO_2 may be evaluated at the average pore radius 11 Å (Table 1) since silica gel has a narrow

TABLE 4
INTRAPARTICLE DIFFUSION OF SO_2 IN SILICA GEL PARTICLES

Temp (°C)	$1/D_e + 5/k_fR$ (sec/cm²)	$5/k_fR$ (sec/cm²)	D_e (cm²/sec)	$\mathscr{D}_K$ (cm²/sec)	$\mathscr{D}_{SO_2}$-He (cm²/sec)	Apparent tortuosity factor, τ_a	Surface diffusivity D_s (cm²/sec)	$\frac{\rho_p K_A D_s}{\beta \mathscr{D}_K/\tau}$
200	1100	2 to 9[a]	0.88×10^{-3}	2.90×10^{-3}	1.12	1.6	4.0×10^{-5}	1.1
235	1000	2 to 9[a]	1.0×10^{-3}	3.01×10^{-3}	1.25	1.5	7.2×10^{-5}	1.3
270	1000	2 to 9[a]	0.91×10^{-3}	3.10×10^{-3}	1.39	1.5	9.5×10^{-5}	1.0

[a] $5/(k_fR) = 2.2$ for $R = 0.540$ mm, 3.7 for $R = 0.272$ mm and 8.6 for $R = 0.114$ mm.

pore-size distribution. Then all the quantities in Eq. (13) are known except D_s. The results for D_s and the ratio of surface to pore-volume diffusion, $\rho_p K_A D_s/[(\beta \mathscr{D}_K)/\tau]$ are given in the final two columns of Table 4. The ratio indicates that surface diffusion and pore-volume diffusion contribute about equally to intraparticle mass transfer. While the absolute values of D_s are subject to error, they are of the same order of magnitude as surface diffusivities of physically adsorbed systems. For example, the summary of Schneider and Smith (*11*) reports D_s values 10^{-4} to 10^{-5} cm^2/sec for propane and butanes on silica gel.

SUMMARY

The adsorption rate constants and heat of adsorption found for SO_2 on silica gel are intermediate between similar results published for physical and for chemisorption. However, the rate was rapid enough that equilibrium was achieved in the time period (10–100 sec) of the chromatographic runs and the adsorption capacity (equilibrium constants) was relatively high. This information, plus the presence of some surface diffusion, suggests that the adsorbed molecules were not strongly bound to the surface. On the other hand, the activation energy for adsorption was high (7.8 kcal/mole) and the extent of surface diffusion was less than that reported for systems exhibiting purely physical adsorption, such as benzaldehyde on activated carbon and on Amberlite (*12,13*). For these reasons it is concluded that SO_2 is held on the sites by bonds of moderate strength, but that the adsorbed molecules are not completely immobile. The SO_2–silica gel system at 175–270°C might be classified as intermediate between purely physical and purely chemisorption. The preliminary measurements at 30 to 150°C where the adsorption was nearly irreversible indicated that the adsorption bond was not as weak as would be ascribed to physical adsorption.

The results obtained at 200 to 270°C (Fig. 7) show that intraparticle diffusion is more important than the intrinsic rate at a site for adsorption (or desorption), except for very small particles. The preliminary experiments indicated that equipment for SO_2 desorption from silica gel would have to operate at temperatures in this same range. Hence, accurate values of the effective diffusivity D_e are needed for proper design.

ACKNOWLEDGMENTS

One of the authors received a grant from the Program of Cultural Cooperation Between United States and Spain. Also financial support from the National Science Foundation is acknowledged.

REFERENCES

1. Jones, W. J., and Ross, R. A., *J. Chem. Soc.* 1021 (1967).
2. Schneider, P., and Smith, J. M., *AIChE J.* **14,** 762 (1968).
3. Masamune, S., and Smith, J. M., *AIChE J.* **11,** 41 (1965).
4. Ma, Y. H., and Marcel, C., *AIChE J.* **18,** 1148 (1972).
5. Suzuki, M., and Smith, J. M., *Chem. Eng. J.* **3,** 256 (1972).
6. Hashimoto, N., and Smith, J. M., *Ind. Eng. Chem. Fundam.* **12,** 353 (1973).
7. Suzuki, M., and Smith, J. M., *J Catal.* **21,** 336 (1971).
8. Wakao, N., Oshima, T., and Yagi, S., *Chem. Eng. Jap.* **22,** 780 (1958).
9. Bird, R. B., Stewart, W. E., and Lightfoot, E. N., "Transport Phenomena," p. 511. Wiley, New York, 1960.
10. Satterfield, C. N., "Mass Transfer in Heterogeneous Catalysis," p. 157. M.I.T. Press, Cambridge, MA, 1970.
11. Schneider, P., and Smith, J. M., *AIChE J.* **14,** 886 (1968).
12. Furusawa, T., and Smith, J. M., *AIChE J.* **20,** 88 (1974).
13. Komiyama, H., and J. M. Smith, *AIChE J.* **20,** 728 (1974).